Volume 21, No 2 | International Journal of Radiation Research, April 2023

NFκB, p53, p21 interacts with DNA damage indicators & Stat3 protein in inducing the radio-modulatory potential of Ethyl cinnamate on HepG2 and BRL3A cells

A. Dutta[1], S. Mukherjee[1], M. Bhattacharyya[2], A. Chakraborty[1*]

[1]UGC-DAE Consortium for Scientific Research, Kolkata Centre LB-8, Sector-III, Salt Lake, Kolkata-700106, India
[2]Department of Biochemistry, University of Calcutta, 35, Ballygunge Circular Road, Kolkata – 700019, India

► ***Original article***

Corresponding author:
Anindita Chakraborty, Ph.D.,
E-mail:
anindita.iuc@gmail.com

Received: March 2022
Final revised: August 2022
Accepted: September 2022

Int. J. Radiat. Res., April 2023; 21(2): 177-187

DOI: 10.52547/ijrr.21.2.1

Keywords: *Radio-sensitization, radio-protection, phytocomponents, ethyl cinnamate, cancer cells, normal cells.*

ABSTRACT

***Background*:** Ethyl cinnamate (Ethyl (2E)-3-phenylprop-2-enoate) is an aromatic compound of cinnamon. According to the Indian Ayurvedic medical system, cinnamon has been used to treat various diseases.The current study examines the potential of ethyl cinnamate (EC) in modulating radiation responses in cancerous (HepG2) and normal (BRL-3A) cells. ***Material & Method*:** HepG2 and BRL3A cells were pre-treated with EC (75 µg/ml) for 24 hours before being subjected to a single 7.5 Gy dose of γ-ray. By using flow cytometry and western blotting, the primarysurvival pathways (PI3-AKT, JAK-STAT, MAPK & JNK), cell cycle inhibitors (p53 & p21), DNA damage indicators (ATM, ATR, γ-H2AX, cleaved PARP), anti-angiogenic TIMP2 and angiogenic factor MMP9 were analysed. The activity of the catalase enzyme was assessed by UV-Visible spectrophotometry. ***Results*:** The complex effects of EC on the suppression of pro-survival and anti-apoptotic proteins such as p-JNK, p-JAK2, p-STAT3, and p-p38MAPK results in enhanced radio-sensitization and radiation-induced cancer cell killing. The radio-response is potentiated by EC's ability to suppress downstream effector proteins such as p21, p-p53, and MMPs and block radiation-triggered p-NF-κB signalling pathways. Additionally, EC effectively enhanced the radio-induced DNA damage in HepG2 cells by stimulating p-ATM, p-ATR, γ-H2AX and PARP cleavage. However, in BRL -3A cells, EC significantly reduced radiation-induced DNA damage. ***Conclusion*:** The potential of EC as a radio-sensitizer in HepG2 cells and a radio-protector in BRL3A cells was observed in this investigation. Based on the elucidated molecular mechanisms, safety profile, and low cost, EC might be considered a promising adjuvant to enhance radio-therapeutic efficacy in cancer treatment.

INTRODUCTION

The development of radio-modulators and radio-recovery agents that can successfully defend against damaging radiation effects has been made possible by advancements in radiation sciences, precisely understanding the effects of ionizing radiation on the biological system. Ionizing radiations interact with biological molecules producing radiolytic products like e (aq), *OH, *H, -OH, +H, O2, and peroxides [1]. These free radicals damage crucial bio-molecules and subsequently inflict harmful effects on the organism [2]. Whole-body exposure to ionizing radiation damages the central nervous system, gastrointestinal tract, and bone marrow. Depending on the total dose and irradiation site, chronic irradiation can lead to cancer, birth anomalies, erythema, and dysfunctions in almost all body organs [3]. Ionizing radiation (IR)-induced cellular damage is implicated in cancer development and treatment. Advancements in radiotherapy have resulted in lower dosage and localization of effects on the tumour; however, radio-resistance in cancer cells and radiation toxicity to normal tissues are still the primary concerns [4]. Research endeavours with synthetic radio-protectors in the past had little success, primarily due to toxicity issues. Therefore, developing radio-protectors and radio-sensitizers from natural products for diverse applications has drawn interest on a global scale [5, 6].

A wide variety of medications used in modern medicine have their origins in natural ingredients [7, 8]. Many plants have been used to mitigate and treat free-radical mediated ailments such as cancer, diabetes, neurodegenerative diseases, etc. [9-12]. Worldwide, scientists have identified several plants that offer effective radioprotection. Numerous plant-derived components have also been found to radio-sensitize tumours, benefiting cancer patients [13]. Understanding the mechanism of actions of radio-modulators requires insight into normal and the cancer cell. ''Normal' cells are the fundamental building elements of the organism and have distinct properties. These characteristics enable them to

[DOI: 10.52547/ijrr.21.2.1]

maintain the proper functioning of the entire biological system. External signals control normal cells, so they only grow and divide when required. They undergo programmed cell death or apoptosis as a part of the normal developmental process and in response to irreversible damages [14, 15]. Normal cells can form selective adhesions, enabling them to remain in their intended location. They differentiate into specialized cells that perform specific functions [16].

Cancer is a genetic illness caused by specific alterations in gene expression in one or more cells [17]. These alterations disrupt homeostasis, which immediately influences cellular growth and division by affecting survival factors such as JAK-STAT, MAPK, and JNK. Cancer cells do not respond to stop signals or cell cycle arresting factors such as p53 and p21, which signal a halt in cell growth and division, resulting in uncontrolled cell proliferation and tumour formation. Typically, the genetic alterations that result in cancer; involve three types of genes; proto-oncogenes, DNA repair genes, and tumour suppressor genes [14, 17]. Therefore, an in-depth understanding of the DNA damage events like PARP cleavage, generation of ATM, ATR, and γ-H2AX is crucial for developing anticancer therapy. Numerous plant polyphenols with antioxidant properties, including curcumin [18, 19], resveratrol [20-22], trans-resveratrol [23], ferulic acid [24, 25] and others, exert radio-modulatory functions on both malignant and normal cells.

Ethyl Cinnamate (EC) is a vital component of cinnamon, although its potential as a phyto-component has not been fully explored. The efficacy of this compound has been unveiled in biological systems such as algae, fungi, and mites [26- 29]; but no significant research has been conducted in higher biological systems to date. The radio-modulatory potential of this bio-active component was studied in HepG2 (cancer) and BRL3A (normal) cells to determine the mechanism of action of EC, with an emphasis on the signalling mediators involved. Therefore the study aims to explore the radio-modulating potential of ethyl cinnamate on both normal and cancer cells to reduce the radiation-induced bystander effect (RIBE) on normal cells while promoting cancer cell death. Since the efficacy of ethyl cinnamate as a radio-modulator has not yet been investigated, this study may introduce another bioactive component that can be used as an adjuvant in the field of radiotherapy to improve the overall outcome of the treatment.

MATERIALS AND METHODS

Materials

HEPES was obtained from Sigma Chemical Co. (St. Louis, MO, USA). The normal liver cell line BRL3A and human hepatocellular carcinoma cell line HepG2 were purchased from NCCS (National Centre for Cell Science), Pune, India. Ethyl Cinnamate (EC) was obtained from Sigma Chemical Co. (St. Louis, MO, USA).Antibody to detect the levels of p-ATM (5883), p -ATR (2853), γ-H2AX (9718), Cleaved PARP (5625), TIMP2 (5738), p-JAK2 (4406), p-STAT3 (9145), p-p38 MAPK (4511), p-SAPK JNK (4668), p-p53 (9286), p21 (2947), p-NFκβ (3033); anti-mouse IgG Fab2 Alexa Fluor 488 (4408) and anti-rabbit IgG Fab2 Alexa Fluor 488 (4412) were purchased from Cell Signalling Technology (Beverly, MA, USA). Cell Counting Kit-8 (96992) was purchased from Sigma-Aldrich (MO, USA). All the cell culture reagents were procured from Gibco Thermo Fisher Scientific (Waltham, MA, USA).

EC and cell lines

Dimethyl sulfoxide (DMSO; 0.1%) was used to prepare the stock solution of EC. Filter sterilization of the stock solution was performed before application. The cell lines were maintained according to the guideline of NCCS (National Centre for Cell Science), Pune, India. Culture of HepG2 and BRL3A cells were carried out in Dulbecco's Modified Eagle's high glucose-containing medium (DMEM), supplemented with 1% antibiotic cocktail solution and 10% fetal bovine serum (FBS) in an atmosphere of 95% air and 5% CO_2 in a 37 °C humidified incubator. Cells were splited in a 1:3 ratio at regular intervals.

CCK8 method for determining cell viability

The HepG2 cells were seeded in 35 mm cell culture plates. Cells were treated with various radiation doses (2Gy, 4Gy, 6Gy, and 7.5Gy) and EC concentrations (10 µg /ml, 25 µg /ml, 50 µg /ml, and 75 µg /ml). By using a combination of radiation and EC at various doses and concentrations, the CCK8 method was used to measure cellular viability. Post-γ -irradiation, the cells were incubated with 150 µl of CCK-8 solution for 2 hours, and then the optical density (OD) value of each plate was measured at 450 nm. The cell survival rate was calculated as the OD value of the experimental group/control group. The method was repeated thrice.

Experimental design

After selecting the dose of EC, radiation, and combination, the cells were divided into four groups:

Control group: HepG2 and BRL3A cells were treated with 0.1% DMSO.

Irradiation group (IR): HepG2 and BRL3A cells were treated with 0.1% DMSO vehicle. After 24 h of vehicle treatment, the cells were exposed to a 7.5 Gy dose of γ-irradiation.

EC (75µg/ml)-treated group: HepG2 cells and BRL3A were treated with 75µg/ml of EC for 24h.

EC (75µg/ml) + Irradiation (IR) group: HepG2 and BRL3A cells were treated with 75µg/ml of EC for 24 h, followed by 7.5 Gy γ-irradiation.

After treatment with EC (75µg/ml) for 24 h, the

[DOI: 10.52547/ijrr.21.2.1]

cells were irradiated with 7.5 Gy of gamma-irradiation (60Co) at the dose rate of 1.2 KGy/hour [PLC based Gamma irradiation System- GC 1200; supplied by Board of Radiation and Isotope Technology, Mumbai, India]. The samples were then incubated in an atmosphere of 5% CO2 and 95% air in a 37 °C humidified incubator. The standard trypan blue exclusion test was carried out to estimate the number of viable cells in each of the above-mentioned experimental groups. All the parameters were studied after 24h of irradiation.

Determination of catalase activity

The cell lysate was added to phosphate buffer (50 mM) (pH -7) containing 100 mM H_2O_2, followed by incubation at 37^0 C for 2 minutes. The absorbance was thoroughly monitored for 5 mins at 240 nm. The alteration in the absorbance with time was directly proportional to the breakdown of H_2O_2. The activity of catalase was expressed as units/mg of protein. One unit of enzyme activity was defined as the quantity of enzyme required to split 1mMole of H_2O_2 into H_2O and O_2 [30].

Cell lysate preparation

Cells were washed with PBS twice; then trypsin-EDTA was added, and the detached cells were collected in precooled centrifuge tubes. Centrifugation was carried out at 3200 rpm for 5 mins at 4^0 C. Supernatant was discarded, and ice-cold RIPA lysis buffer (1 ml/1*10^7 cell) was added to the pellet and mixed well. Constant agitation was maintained for 30 minutes at 4^0 C; then, the lysate was incubated on ice for 15 minutes. The lysate was sonicated thrice with 2 second pulses, with 1 minute rest on ice between each pulse. The cell lysate was vortexed 4-6 times during the incubation. Lysates were incubated in ice for additional 15 minutes. Then it was centrifuged at 12000*g for 20 minutes at 4^0 C. The supernatant, which can be used for experiments as a cell lysate, was collected in a fresh tube kept on ice; and the pellet was discarded.

Western blot assay

In each well of 12% sodium dodecyl sulphate-polyacrylamide gel (SDS-PAGE), an equal amount of protein (50 µg) was loaded. A transfer process into a nitrocellulose membrane was done on completion of the electrophoresis. 5% bovine serum albumin (BSA) solution for 2 h was used in blocking the membrane at 37^0 C. Immunoblot was carried out using the antibodies against p-ATM, p-ATR, γ-H2AX, cleaved PARP, TIMP2, p-p53, p21, p-NFκB, p-JAK2, p-STAT3, p- SAPK JNK, p- p38 MAPK. As a loading control, the β -actin antibody was used. Then the membrane was incubated with primary antibodies for 3 h at room temperature. Then secondary antibody tagged with alkaline phosphatase was added and incubated for 2 h at room temperature. NBT-BCIP solution was applied to visualise the protein bands. The determination of the relative protein levels was done by normalisation of the quantity of internal control proteins. SyngeneGbox EF Gel Documentation System was used to analyse the immunoblots, and *GeneTools software* with *GeneSnap* imaging was used to quantify them. The western blot was carried out three independent times (n = 3) to calculate the mean ± SEM value.

Analysis of protein expression by flowcytometry

The cells were harvested after 24 hr of irradiation and fixed with 4% paraformaldehyde in PBS (pH 7.4). The cells were incubated for 5 min with 0.1% Triton X-100 in PBS for permeabilization. Afterwards, the cells were washed twice with PBS containing 3% FBS and were then incubated with primary antibodies (p-JAK2, p-STAT3, p-p38 MAPK, p- SAPK JNK, TIMP2, p21, p-p53, p-NFκβ, p-ATM, p-ATR & cleaved PARP) for 2 h in ice. Cells were washed with PBS twice. Then the cells were incubated with either Fluorescence tagged anti-rabbit or anti-mouse secondary antibody (depending upon the primary antibody) for 30 mins in ice. Next, to remove the excess unbound secondary antibody from the cells, they were washed with PBS twice. 10,000 cells for each group were acquired and analyzed by BD FACS Calibur equipped with Cell Quest Pro software. The expression of different proteins was checked three independent times (n = 3), to calculate the mean and SEM.

Statistical analysis

The values were given in terms of mean ± standard error of the mean (SEM as error). The one-way analysis of variance (ANOVA) with Tukey's post hoc test was carried out for statistical evaluation of the data. A value of $p < 0.05$ was considered significant in all the cases. The significance of differences '**' was calculated between the control vs. combination (IR+EC) group and '#', '##'irradiation vs. combination (IR+EC) group. '**' and '##' indicated $p < 0.01$ while '#' indicated $p < 0.05$.

RESULT

The effect of EC on cell viability of HepG2 cells (CCK8 method)

Figure 1 depicts that cell viability was highest in the untreated HepG2 cells. The results showed that the IC50 concentration of EC was 75 µg /ml (figure 1B), and the LD50 radiation dose was 7.5 Gy (figure 1A). Lower EC concentrations (10 µg /ml, 25 µg /ml, 50 µg /ml) had no significant effect on lower radiation dose (2Gy, 4Gy, 6Gy) (figure 1C) exposed cells. Therefore, a combination of the IC50 concentration and the LD50 dose was chosen for the studies.

Impact of EC on p-p53 and p21

Under different experimental settings (EC, IR, and IR+EC), HepG2 cells showed higher effects on the

[DOI: 10.52547/ijrr.21.2.1]

expression of tumour suppressor, cell cycle inhibitor – p- p53 than the anti-proliferative effector – p21. The p-p53 level increased 2.24-fold after EC treatment, whereas the level of p21 increased only 1.36-fold (figure 2C). Similarly, HepG2 cells exposed to γ-rays demonstrated a 3.3-fold rise in p-p53 expression compared to a 2.59-fold increase in p21 expression. In contrast, the combination treatment of IR and EC had the most significant effect on p21 and p-p53. Compared to untreated cells, IR+EC treatment increased p21 expression by 3.34-fold and p53 expression by 4.74-fold. When compared to irradiated cells, the IR+EC treatment increased the levels of p53 and p21 by 42% and 29%, respectively (figure 2C).

In the BRL-3A cells, EC alone had no significant ($p < 0.01$) effect on the expression levels of both p-p53 and p21. However, when combined with IR, EC significantly reduced the radio-induced levels of both p21 and p-p53. Exposure of BRL-3A cells to γ-radiation sharply elevated the expression of both p21 (↑ 2.49-fold) and p-p53 (↑ 5.17-fold), compared to the other experimental groups – EC (↓ 1.18-fold: p21) (↑ 1.37-fold: p-p53) and IR+EC (↑ 1.59-fold: p21) and (↑ 3.07-fold: p-p53) (figure 2D). EC administration reduced the radio-induced expression of p21 and p-p53 by 63.84% and 59.38%, respectively.

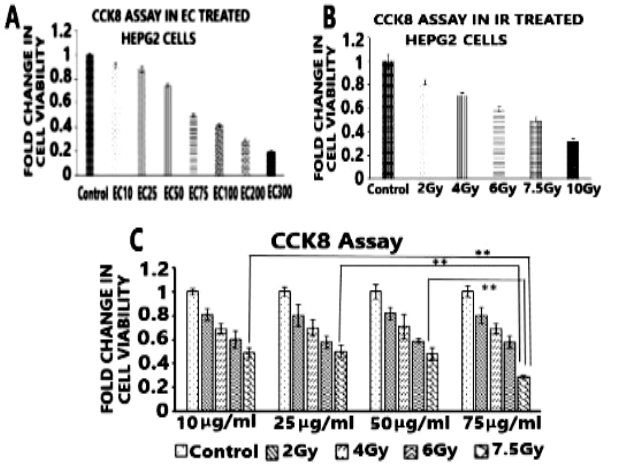

Figure 1. Radiation induced effects on cellular viability of γ-irradiated HepG2 cells pretreated with EC. **(A)** HepG2 cells were exposed to different doses of radiation (2, 4, 6, 7.5, 10 Gy). **(B)** HepG2 cells were exposed to different concentrations of EC (10, 25, 50, 75, 100, 200, 300 µg/ml). **(C)** HepG2 cells were exposed to combinations of different radiation doses and EC concentrations. Error bars were SEM for n=3, $p<0.01$ was considered significant. Statistical comparison was done between 10 µg/ml + 7.5 Gy vs. 75 µg/ml + 7.5 Gy, 25 µg/ml + 7.5 Gy and 50 µg/ml + 7.5 Gy designated by '**' ($p<0.01$).

EC upregulates TIMP2 and suppresses MMP9

TIMP2, a well-known metastasis suppressor, was down-regulated by γ-rays compared to untreated HepG2 cells, whereas EC markedly increased TIMP2 expression independently and in conjunction with radiation. The expression of TIMP2 increased 1.22-fold when the cells were exposed to EC alone. After irradiation, TIMP2 levels were 1.58-times lower than in untreated cells (figure 3B). Thus, compared to the radiation-exposed cell population, TIMP2 expression increased by 94% in EC-exposed cells. IR+EC treated cells had a 3.37-fold increase in TIMP2 levels compared to irradiated HepG2 cells.

In addition to up-regulating TIMP2 expression, the combination of EC and γ-rays significantly ($p < 0.01$) reduced (↓ 56.08% than IR group) the radio-induced expression of MMP9, one of the critical angiogenic factors, in HepG2 cells. MMP9 expression was up-regulated by 31.26% when cell was exposed to γ-rays individually. In figure 3 (D), the expression percentage of TIMP2 and MMP9 in the IR+EC group demonstrates the radio-sensitizing efficacy of the combined treatment against HepG2 cells.

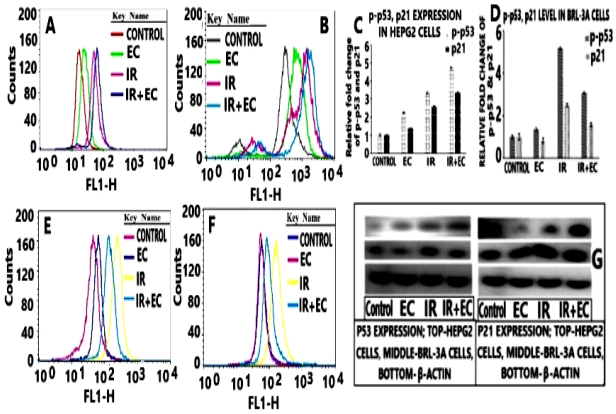

Figure 2. (A)(B) The overlaid histogram plots represented respectively the level of p21 &p-p53 in different experimental groups of HepG2 cells. Along the X-axis intensity of Alexa Flour 488 in FL1-H (Alexa Flour 488) channel and along the Y-axis count was taken. **(C)(D)** The bar diagrams represented the relative fold change of p-p53 & p21 in different experimental conditions respectively in HepG2 & BRL-3A cells. **(E)(F)** The overlaid histogram plots represented respectively the level of p-p53 & p21 in different experimental groups of BRL-3A cells. Along the X-axis intensity of Alexa Flour 488 in FL1-H (Alexa Flour 488) channel and along the Y-axis count was taken. **(G)** The western blot images of p-p53 expression under different experimental conditions in HepG2 and BRL-3A (left) and p21 expression (right) in HepG2 and BRL-3A cells. Error bars were SEM for n = 3.

Effect of EC on prime cellular survival pathways

The expression of one of the most critical cell survival pathways, p-JNK, increased after HepG2 cells were exposed to γ-radiation (7.5 Gy). Individual administration of EC (75µg/ml) reduced the expression levels compared to irradiated cells but did not result in a significant reduction ($p < 0.05$) compared to untreated cells. EC alone induced a 2.02% decrease in p-JNK than control cells, whereas irradiation caused an 8.22% elevation. When HepG2 cells were exposed to both IR and EC, there was a decline in p-JNK expression (15.14% ↓) (figure 4D). However, none of the treatments made any significant alteration in the expression level of p-JNK in HepG2 cells.

In addition to radio-sensitizing cancer cells, EC protects normal cells from γ-rays by inhibiting the radio-induced down-regulation of the critical survival

[DOI: 10.52547/ijrr.21.2.1]

pathways. Exposure of BRL-3A cells to γ-rays sharply down-regulated the p-JNK expression by 67.38. However, EC pre-treatment efficiently counteracted the radio-induced suppression of p-JNK, significantly boosting expression by 42.83% ($p < 0.05$) (figure 4E).

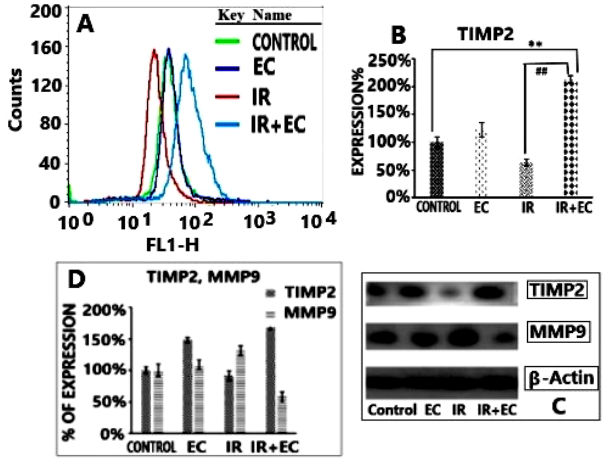

Figure 3. (A) The overlaid histogram plot represented the level of TIMP2 in different experimental groups of HepG2 cells. Along the X-axis intensity of Alexa Flour 488 in FL1-H (Alexa Flour 488) channel and along the Y-axis count was taken. **(B)** The bar diagram represented the percentage (%) of TIMP2 expression under different experimental conditions in HepG2 cells. **(C)** The western blot images of TIMP2 expression under different experimental conditions in HepG2 cells. **(D)** The bar diagram represented the relative expression% of TIMP2 & MMP9 under different experimental conditions in HepG2 cells. Error bars were SEM for n = 3. p< 0.01 was considered significant. Statistical comparison was done between control vs. IR+EC designated by '**' and IR vs. IR+EC designated by '##' in figure.

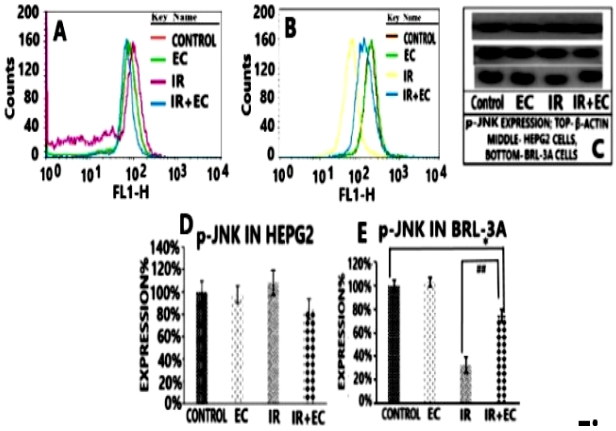

Figure 4. IR+EC reduced p-JNK in HepG2 cells and prevented radio-induced decrease in BRL-3A cells. **(A)** The overlaid histogram plot represented the level of p-JNK in different experimental groups of HepG2 cells. Along the X-axis intensity of Alexa Flour 488 in FL1-H (Alexa Flour 488) channel and along the Y-axis count was taken. **(B)** The overlaid histogram plot represented the level of p-JNK in different experimental groups of BRL-3A cells. **(C)** The western blot images of p-JNK expression under different experimental conditions in HepG2 and BRL-3A. **(D) (E)** The bar diagrams represented the percentage (%) of expression of p-JNK in different experimental conditions respectively in HepG2 and BRL-3A cells. Error bars were SEM for n = 3. .p< 0.05 (* or #) & p< 0.01 was considered significant. Statistical comparison was done between control vs. IR+EC designated by '**' and IR vs. IR+EC designated by '##' in figure.

Two crucial survival factors, p-JAK2 and p-STAT3, were differentially affected by radiation in HepG2 cells. After irradiation, there was a 9.31% increase in p-STAT3 expression but a 33.4% decrease in p-JAK2 expression (figure 5C & D). EC alone had a considerable influence on p-JAK2 and p-STAT3 expression. EC significantly down-regulated the expression of p-JAK2 (↓ 32.46%) andp-STAT3 (↓ 48.56%). Moreover, when used in combination (EC + radiation), EC dramatically reduced the effect of radiation on p-STAT3 expression (↓ 73.85%). In the case of p-JAK2, EC boosted the individual effects of both EC and IR. Following IR+EC treatment p-JAK2 expression was reduced by 45.25%.

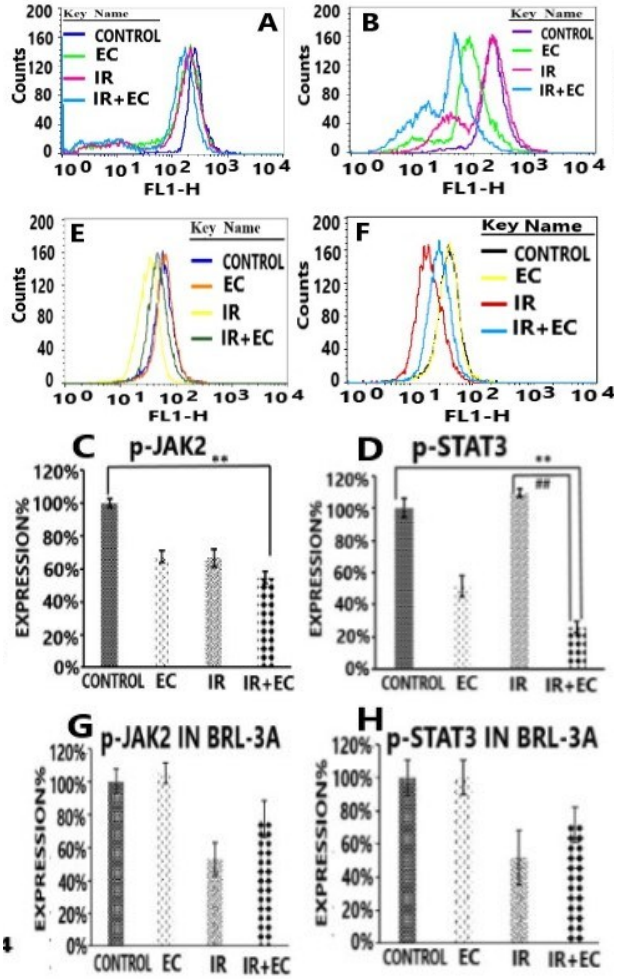

Figure 5. IR+EC downregulated p-JAK2 and p-STAT3 in HepG2 cells and prevented radio-induced reduction in BRL-3A cells. **(A) (B)** The overlaid histogram plots represented respectively the level of p-JAK2 and p-STAT3 in different experimental groups of HepG2 cells. Along the X-axis intensity of Alexa Flour 488 in FL1-H (Alexa Flour 488) channel and along the Y-axis count was taken. **(C) (D)** The bar diagrams represented respectively the percentage (%) of expression of p-JAK2 and p-STAT3 in different experimental conditions in HepG2 cells. **(E) (F)** The overlaid histogram plots represented respectively the level of p-JAK2 and p-STAT3 in different experimental groups of BRL-3A cells. **(G) (H)** The bar diagrams represented respectively the percentage (%) of expression of p-JAK2 and p-STAT3 in different experimental conditions in BRL-3A cells. Along the X-axis intensity of Alexa Flour 488 in FL1-H (Alexa Flour 488) channel and along the Y-axis count was taken. Error bars were SEM for n = 3. . p< 0.01 was considered significant. Statistical comparison was done between control vs. IR+EC designated by '**' and IR vs. IR+EC designated by '##' in figure.

[DOI: 10.52547/ijrr.21.2.1]

However, radiation exposure had no effect on p-STAT3 expression in BRL-3A cells while significantly ($p < 0.01$) reducing p-JAK2 expression. γ-rays resulted in a 3.36-fold reduction in p-JAK2 levels in the case of BRL-3A cells. Pre-treatment with EC impedes the radio-induced reduction of p-JAK2 and p-STAT3 expression, boosting p-JAK2 expression by 7.28% and p-STAT3 expression by 5.72% (figure 5G & H).

Radiation exposure (7.5 Gy) increased the expression of another important survival pathway, p-p38 MAPK, by 14% in HepG2. However, EC alone caused a significant ($p < 0.01$) reduction (↓ 35.59%) compared to untreated HepG2 cells (figure 6B). When combined with radiation, EC completely counteracted the survival-enhancing effect of radiation by inhibiting p-p38 MAPK expression significantly ($p < 0.01$). The p-p38 MAPK level in HepG2 cells was reduced by 69.15% after IR+EC treatment.

Irradiated BRL-3A cells showed a sharp decrease (50.2% ↓) in the p-p38 MAPK expression, whereas EC -treated cells showed an up-regulation of 24.73% (figure 6D). Moreover, EC pre-treatment inhibited the down regulation of p-p38 MAPK, increasing it by ↑ 34.13%.

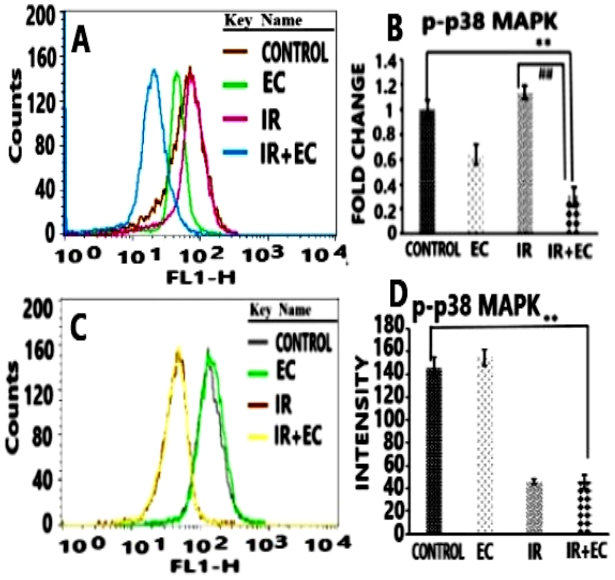

Figure 6. IR+EC downregulated p-p38 MAPK in HepG2 & BRL-3A cells. **(A)** The overlaid histogram plot represented the level of p-p38 MAPK in different experimental groups of HepG2 cells. Along the X-axis intensity of Alexa Flour 488 in FL1-H (Alexa Flour 488) channel and along the Y-axis count was taken. **(B)** The bar diagram represented the fold change in the expression of p-p38 MAPK in different experimental conditions in HepG2 cells. **(C)** The overlaid histogram plot represented the level of p-p38 MAPK in different experimental groups of BRL-3A cells. **(D)** The bar diagram represented the intensity of expression of p-p38 MAPK in different experimental conditions in BRL-3A cells. Along the X-axis intensity of Alexa Flour 488 in FL1-H (Alexa Flour 488) channel and along the Y-axis count was taken. Error bars were SEM for n = 3. . $p < 0.01$ was considered significant. Statistical comparison was done between control vs. IR+EC designated by '**' and IR vs. IR+EC designated by '##' in figure.

Alteration in p-NFκβ signalling with EC in HepG2 and BRL3A cells

Radiation significantly ($p < 0.01$) increased the expression of p-NFκβby 30% in HepG2 cells (figure 7B). EC inhibited p-NFκβ activation when used alone or in combination with radiation. EC alone caused a 36.06% reduction in the expression level of p-NFκβ. Combination with radiation accelerated EC impact and blocked the radio-induced activation of p-NFκβ. IR+EC treatment in HepG2 cells caused a 43.63% decrease in the expression level of p-NFκβ.

Irradiation of BRL-3A cells resulted in a sharp increase in p-NFκβ expression, with a nearly 4-fold increase in the irradiated cells (figure 7D). On the other hand, pre-treatment with EC significantly reduced p-NFκβ expression in irradiated BRL3A cells, resulting in a2-fold decrease.

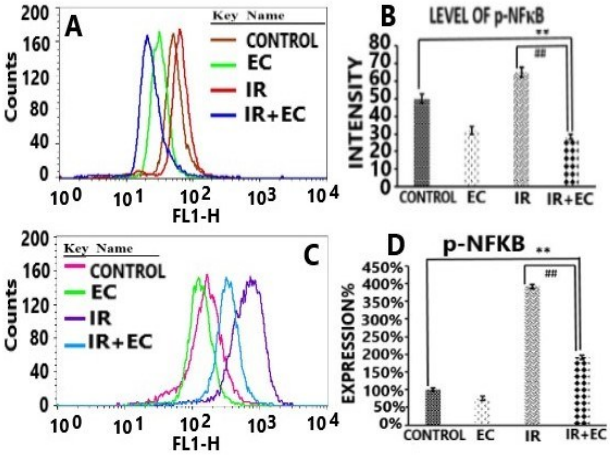

Figure 7. IR+EC downregulated p-NFκβin HepG2 & BRL-cells. **(A)** The overlaid histogram plot represented the level of p-NFκβ in different experimental groups of HepG2 cells. Along the X-axis intensity of Alexa Flour 488 in FL1-H (Alexa Flour 488) channel and along the Y-axis count was taken. **(B)** The bar diagram represented the p-NFκβ intensity in different experimental conditions in HepG2 cells. **(C)** The overlaid histogram plot represented the level of p-NFκβ in different experimental groups of BRL-3A cells. **(D)** The bar diagram represented the percentage of expression of p-NFκβ in different experimental conditions in BRL-3A cells. Along the X-axis intensity of Alexa Flour 488 in FL1-H (Alexa Flour 488) channel and along the Y-axis count was taken. Error bars were SEM for n = 3. . $p < 0.01$ was considered significant. Statistical comparison was done between control vs. IR+EC designated by '**' and IR vs. IR+EC designated by '##' in figure.

EC accelerates PARP cleavage in HepG2 cells and inhibits it in BRL3A cells

One of the primary cell death events, PARP cleavage, was up-regulated at varying rates under several experimental settings (EC, IR, IR+EC).The cleaved PARP intensity gradually increased in EC, IR and IR+EC treated HepG2 cells. Application of EC caused a 1.34-fold increase in the cleaved PARP level, whereas radiation exposure induced a 1.93- fold up-regulation (figure 8C). However, EC, in combination with radiation, accelerated the individual impacts of EC and IR on the cleaved PARP expression. IR+EC treatment significantly ($p < 0.01$) elevated the cleaved

[DOI: 10.52547/ijrr.21.2.1]

PARP level (↑ 3.17 fold).

In BRL-3A cells, the opposite trend was observed in different experimental groups (EC, IR, IR+EC). Irradiation increased PARP cleavage significantly (↑ 3.57 fold), whereas EC alone and combined with γ-rays successfully reduced cleaved PARP levels (figure 8E). Individual application of EC resulted in 18.95% down-regulation compared to the control BRL-3A cells, whereas pre-treatment with EC effectively prevented the radio-induced PARP cleavage (↓ 1.71 fold than IR).

Impact of EC on p-ATM and p-ATR

All experimental conditions increased the expression of both p-ATM and p-ATR in HepG2 cells, though the rate of increase varied greatly. In these cells, EC and IR, individually or in combination, had a higher impact on p-ATM than p-ATR. Individual application of EC resulted in a 33.92% increase in p-ATM level and a 25.07% rise in p-ATR expression (figure 9 C & D). Radiation exposure significantly increased p-ATM level (59.8%), although only a 28.22% increase in p-ATR was found. When HepG2 cells were exposed to IR+EC treatment, p-ATR levels increased by 40.7%, while p-ATM levels increased by 71.78%.

Radiation exposure significantly elevated both p-ATM and p-ATR in BRL-3A cells. Irradiated BRL-3A cells showed a 5.17-and 4.9-fold increase in p-ATM and p-ATR, respectively (figure 9 E & G). Although EC alone did not significantly affect both p-ATM and p-ATR, when combined with γ-rays, it efficiently counteracted the surge in their (p-ATM and p-ATR) expression. Compared to untreated BRL-3A cells, EC + radiation treatment generated a 2.72 fold decrease in p-ATM expression and a 2.22 fold reduction in p-ATR level.

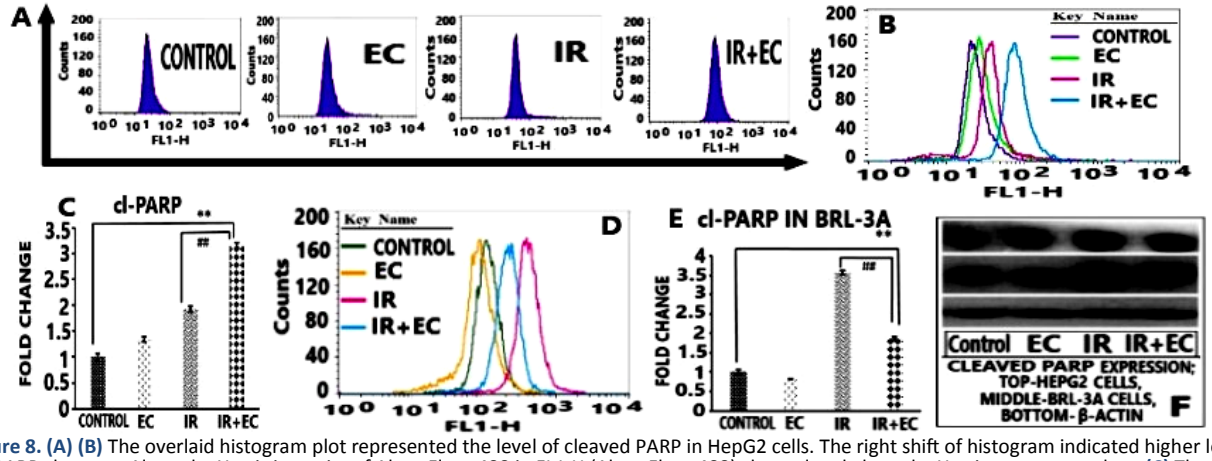

Figure 8. (A) (B) The overlaid histogram plot represented the level of cleaved PARP in HepG2 cells. The right shift of histogram indicated higher level of PARP cleavage. Along the X-axis intensity of Alexa Flour 488 in FL1-H (Alexa Flour 488) channel and along the Y-axis count was taken. **(C)** The bar diagram represented the fold change of cleaved PARP expression under different experimental conditions in HepG2 cells. **(D)** The overlaid histogram plot represented the level of cleaved PARP in BRL-3A cells. Along the X-axis intensity of Alexa Flour 488 in FL1-H (Alexa Flour 488) channel and along the Y-axis count was taken. **(E)** The bar diagram represented the fold change of cleaved PARP expression under different experimental conditions in BRL-3A cells. Error bars were SEM for n = 3. p< 0.01 was considered significant. Statistical comparison was done between control vs. IR+EC designated by '**' and IR vs. IR+EC designated by '##' in figure. **(E)** The western blot images of cleaved PARP expression in HEPG2 and BRL-3A cells.

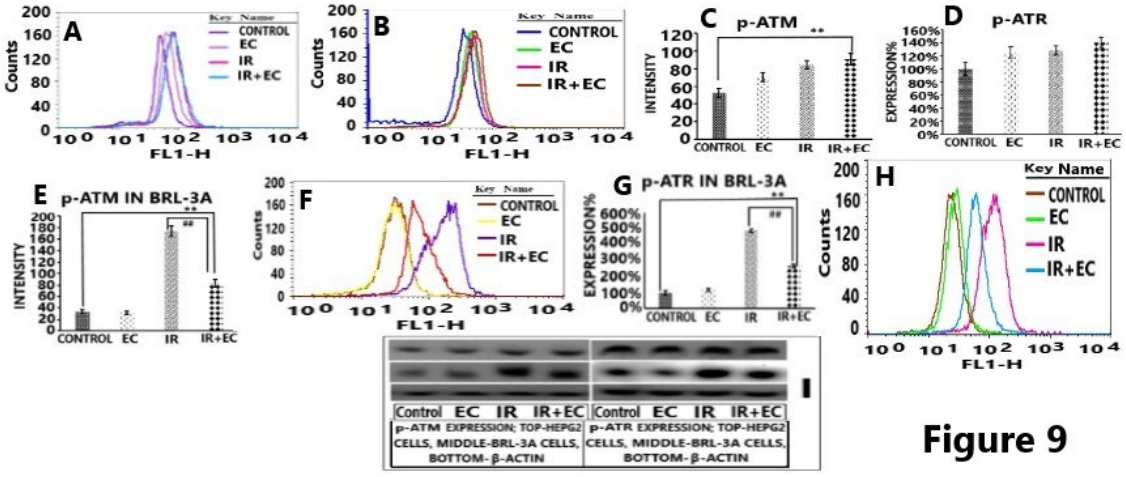

Figure 9

Figure 9. IR+EC increased p-ATM & p-ATR level in HepG2 cells and hinders the IR-induced rise in BRL-3A cells: **(A) (B)** The overlaid histogram plots represented respectively the level of p-ATM & p-ATR in HepG2 cells. The right shift of histogram indicated higher level of expression. Along the X-axis intensity of Alexa Flour 488 in FL1-H (Alexa Flour 488) channel and along the Y-axis count was taken. **(C) (D)** The bar diagrams represented respectively the intensity of p-ATM & the percentage (%) and of p-ATR expression under different experimental conditions in HepG2. **(E)** The bar diagram represented the intensity of p-ATM expression in BRL-3A cells. **(F)** The overlaid histogram plot represented the level of p-ATM in HepG2 cells. Along the X-axis intensity of Alexa Flour 488 in FL1-H (Alexa Flour 488) channel and along the Y-axis count was taken. **(G)** The bar diagram represented the intensity of p-ATR expression in BRL-3A cells. Error bars were SEM for n = 3. . p< 0.01 was considered significant. Statistical comparison was done between control vs. IR+EC designated by '**' and IR vs. IR+EC designated by '##' in figure. **(H)** The overlaid histogram plot represented the level of p-ATM in HepG2 cells. Along the X-axis intensity of Alexa Flour 488 in FL1-H (Alexa Flour 488) channel and along the Y-axis count was taken. **(I)** The western blot images of p-ATM expression (left) & p-ATR expression (right) in HEPG2 and BRL-3A cells.

[DOI: 10.52547/ijrr.21.2.1]

EC increases γ-H2AX generation in HepG2 cells and prevents it in BRL3A cells

Different experimental conditions (EC, IR, IR+EC) resulted in different levels of up-regulation of γ-H2AX formation in HepG2 cells. Irradiation markedly elevated the expression of γ-H2AX (↑ DNA damage), whereas EC treatment resulted in no significant effect. Exposure of HepG2 cells to γ-radiation resulted in a 28.94% rise in the γ-H2AX level (figure 10 C). However, EC sharply accelerated the generation of γ-H2AX when combined with radiation. The combination (EC+radiation) treatment increased the expression of γ-H2AX by 69.59%.

Following irradiation, BRL-3A cells showed a 9.6-fold increase in γ-H2AX formation (figure 10 D). Application of EC before radiation exposure provided significant radioprotection. EC+radiation significantly reduced (↓ 5.71 fold) γ-H2AX generation.

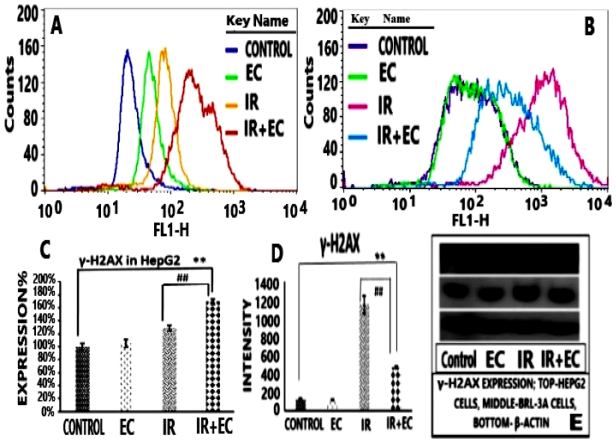

Figure 10. IR+EC increased γ-H2AX level in HepG2 cells and hinders the IR-induced rise in BRL-3A cells: **(A) (B)** The overlaid histogram plots represented the level of γ-H2AX respectively in HepG2 and BRL-3A cells. The right shift of histogram indicated higher level of γ-H2AX. Along the X-axis intensity of Alexa Flour 488 in FL1-H (Alexa Flour 488) channel and along the Y-axis count was taken. **(C) (D)** The bar diagrams represented respectively the percentage (%) and intensity of γ-H2AX expression under different experimental conditions in HepG2 & BRL-3A cells. Error bars were SEM for n = 3. . p< 0.01 was considered significant. Statistical comparison was done between control vs. IR+EC designated by '**' and IR vs. IR+EC designated by '##' in figure. **(E)** The western blot images of γ-H2AX expression in HEPG2 and BRL-3A cells.

Effect of EC on catalase activity

Catalase activity was higher in EC-treated HepG2 cells (29.25 moles of H_2O_2 reduced/ mg of protein/ min) than in irradiated (7.5 Gy) cells (22.4 moles of H_2O_2 reduced/ mg of protein/ min) (figure 11 A). However, these experimental groups had significantly lower catalase activity (36.4 moles of H_2O_2 reduced/ mg of protein/ min) than untreated HepG2 cells. The combined effects of EC (75 g/ml) and IR (7.5 Gy) significantly reduced the catalase activity (15.7 moles of H_2O_2 reduced/ mg of protein/ min) in HepG2 cells.

However, EC had the opposite effect in BRL-3A cells. Pre-treatment with EC (75μg/ml) markedly counteracted the radio-induced decreasein catalase activity. The catalase activity was significantly reduced after irradiation (7.5 Gy) (21.49 moles of H2O2 removed/ mg of protein/ min) (figure 11 B). However, EC treatment before radiation exposure, considerably restored catalase activity (35.93 μmoles of H_2O_2 reduced/ mg of protein/ min), indicating its radio-protective potential.

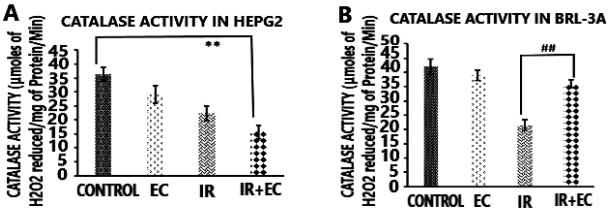

Figure 11. (A) (B) The bar diagrams represented the catalase activity (μmoles of H2O2 reduced/ mg of Protein/ Min) in different experimental conditions respectively in HepG2 and BRL-3A cells. Error bars were SEM for n = 3. p< 0.01 was considered significant. Statistical comparison was done between control vs. IR+EC designated by '**' and IR vs. IR+EC designated by '##' in figure.

DISCUSSION

The current investigation reveals the modulatory effects of EC on radio-induced intracellular perturbations that alter cellular homeostasis. The present study assesses damage using key signalling molecules of cellular metabolism, inflammation, and DNA damage indicators.

EC effectively reduced radio-induced DNA damage in BRL-3A cells, although it increased in HepG2 cells. PARP cleavage is a critical indicator of DNA damage and apoptosis [31]. Plant polyphenols such as ferulic acid [32] and ellagic acid [33] have been shown to up-regulate PARP cleavage in U-87 MG glioblastoma cell line and PC3 prostate cancer cell line, respectively. Similar to the earlier findings; in this study, the combination of EC and IR markedly increased the cleaved PARP intensity in HepG2 cells, triggering apoptosis. The exact opposite was true for BRL-3A cells, where EC prevented radio-induced PARP cleavage and protected normal cells from radio -induced DNA damage. Both ATM and ATR are activated by DNA damage and replication stress [32].Furthermore, ATM and ATR often work together to detect DNA damage and regulate downstream processes [34].

In a previous investigation, resveratrol, a polyphenolic phytoalexin [35], showed radio sensitizing activities in PC3 prostate cancer cells by accelerating DNA double strand breaks (DSB) and activating ATM/Chk1 pathway. In another study [36] curcumin had a comparable effect in pancreatic adenocarcinoma cell line BxPC-3. In HepG2 cells, EC significantly increased the radio-induced generation of ATM without affecting ATR production. However, in BRL-3A cells, EC significantly reduced the radio-induced yield of ATM and ATR potentially exerting radioprotection on normal cells. DNA

[DOI: 10.52547/ijrr.21.2.1]

damage, whether endogenous or exogenous, causes double-stranded breaks (DSBs) and is always followed by phosphorylation of the histone H2AX. H2AX is a variant of the H2A protein family, a component of the histone octamer in nucleosomes. It is phosphorylated by kinases such as ataxia telangiectasia mutated (ATM) and ATM-Rad3-related (ATR) in the PI3K pathway [37].

In an earlier study [35] resveratrol was found to have a potential radio sensitizing effect on DAB2IP-deficient prostate cancer cell lines LAPC4-KD and PC3-KDby up-regulating DNA damage and boosting γ -H2AX generation. Similarly [38] curcumin also exerted significant radio sensitization in two pancreatic cell lines, Panc-1 and MiaPaCa-2, by stimulating γ-H2AX formation. In our study, EC alone had minimal impact on γ-H2AX production, but when combined with radiation, it greatly enhanced γ-H2AX formation in HepG2 cells. This further supports the potential of IR+EC in causing DNA damage in cancer cells. Moreover, in BRL-3A cells, EC effectively inhibited radio-induced up-regulation of γ-H2AX expression, confirming EC as a potent radio-protective agent in normal cells. In mammalian cells, DNA damage frequently triggers the p53-p21 pathway, resulting in G (1)-phase arrest [39]. By activating p53 and p21, the plant polyphenol, quercetin, significantly radio sensitized HepG2 cells [40]. Resveratrol sensitized the radioresistant prostate cancer cell lines LAPC4-KD and PC3-KD by increasing p53expression [41]. Ellagic acid remarkably induced the activity of both p53 and p21 in human bladder cancer T24 cells. In HepG2 cells,we found that EC, IR, and IR+EC treatments graduallyincreased p21 and p53 levels. DNA damaging events could cause this enhancement. After radiation exposure, both p53 and p21 were significantly up-regulated in BRL-3A cells. However, EC effectively inhibited the radio-induced acceleration of p53 and p21 expression in BRL-3A cells. These findings added to the evidence that EC can promote cancer cell death by activating DNA damage-dependent cell cycle arresting proteins, such as p53 and p21, and effectively protect normal cells from radiation damage.

Catalase is an antioxidant enzyme found in all major organs of our body. Earlier research [42, 43] suggested inhibiting catalase activity could be associated with cancer cell death [44]. By lowering catalase activity, ferulic acid significantly increased radio sensitization in HeLa and ME-180 cells, two human cervical cancer cell lines. We observed marked suppression of catalase activity in HepG2 cells treated with a combination of IR and EC. Reduced catalase activity inevitably increases intracellular oxidative stress, which may contribute to DNA damage and induce apoptosis. However, in normal cells (BRL-3A), EC significantly counteracted the radio-induced down-regulation of catalase activity, reducing the occurrence of DNA damage. This suggests that EC can be an effective radio-protector in normal cells.

The JNK and p38 MAPK pathways regulate the activity and expression of key inflammatory mediators, such as cytokines and proteases, which may act as cancer promoters [45]. Tea catechins have been reported to promote cytotoxicity of human T lymphocytic leukaemia Jurkat cells by activating the JNK/IFN-γ pathway in a hydrogen peroxide-dependent or independent manner [46]. Furthermore, curcumin induced apoptosis in osteosarcoma MG63 cells by down-regulating the c-Jun N-terminal kinase (JNK) signalling pathway, which is involved in autophagy [47]. In contrast, under various experimental conditions in this investigation, no appreciable changes in JNK expression were seen in HepG2 cells. However, in BRL-3A cells, irradiation caused significantly reduced JNK expression, which EC effectively counteracted. Our study found that EC significantly reduced the radio-induced increase in MAPK expression in HepG2 cells. Similarly, EC protected the BRL-3A cells from the radio-induced suppression of MAPK expression. The JAK/STAT pathway regulates stem cell maintenance, haematopoiesis, and the inflammatory response. The pathway transduces signals from cytokines, interleukins, and growth factors that act through several transmembrane receptor families [48].

In a previous investigation [49] through the inhibition of Stat3 activation, resveratrol demonstrated strong anticancer effects in two ovarian cancer cell lines, CAOV-3 and OVCAR-3 cells. In human epidermoid carcinoma cell line-A431 cells, resveratrol significantly inhibited JAK phosphorylation. This suppressed STAT1 phosphorylation, leading to down-regulation of JAK/ STAT-mediated gene transcription and accelerating the mitochondrial cell death pathway [50].

In this study, radiation exposure had varied effects on JAK and STAT expressions in HepG2 cells. JAK expression was downregulated in irradiated HepG2 cells, but STAT expression was elevated. Nevertheless, radiation exposure significantly reduced JAK and STAT expressions in BRL-3A cells. EC efficiently inhibited the radio-induced down-regulation of JAK and STAT expression. Thus, EC acts as a radio-sensitizer in cancer cells and a radio-protector in normal cells, imparting anti-survival effects in HepG2 cells and pro-survival effects in BRL-3A cells. Inflammation is a hallmark of cancer and plays a critical role in the development and progression of most malignancies. NFκB is a crucial signalling pathway linked to the emergence and spread of cancer [51]. NFκB regulates tumour cell proliferation, survival, and angiogenesis by modulating the expression of target genes, such as TNFA, IL6, BCLXL, BCL2, BCLXS, XIAP, and VEGF [52, 53]. In different hepatocellular carcinoma cell lines- PLC, KMCH, and Huh7 cells, curcumin treatment has exhibited significant anticancer activities by suppressing NFκB signalling [54].

[DOI: 10.52547/ijrr.21.2.1]

According to our findings, radiation exposure significantly increased the level of NFκB in both cancer and normal cells. EC inhibited the radio-induced accelerated expression of NF-κB in HepG2 and BRL-3A cells. Therefore, EC combinedwith radiation aids in the prevention of angiogenesis and cancer cell metastasis.

Tissue inhibitors of metalloproteinases (TIMPs) are endogenous proteins that restrict cell proliferation and migration by inhibiting the function of matrix metalloproteinases (MMPs) [55]. Tissue inhibitor of metalloproteinase-2 (TIMP-2) is a unique TIMP inhibitor family member because it is implicated in tumour growth, inflammation, and other diseases and correlates with matrix remodelling and angiogenesis suppression [56]. In a previous investigation on human bladder cancer cell line T24 cells, curcumin had an effective anticancer effect by suppressing the matrix metalloproteinase signalling pathway by deactivating MMP2, MMP9 and boosting TIMP2 activity [57]. Interestingly, in this study, EC individually and in combination with γ-radiation significantly increased TIMP2 expression. Thus, in combination with radiation, EC effectively prevented angiogenic and related factors, leading to a marked reduction in metastatic events.

These data further established EC as a robust natural radio-sensitizer in cancer cells (HepG2) and a potent radio-protector in normal BRL-3A cells.

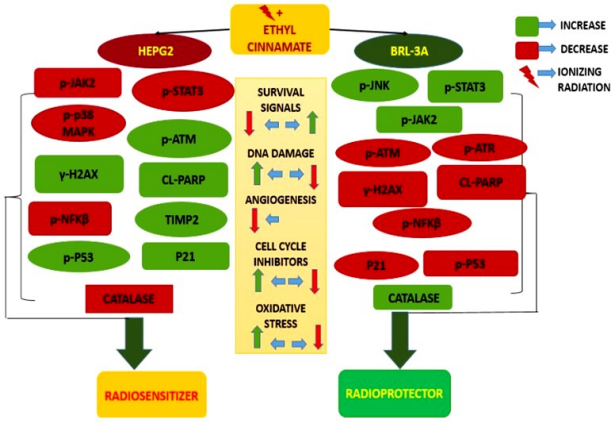

Figure 12. Schematic diagram of the hypothetical working mechanism. The diagram represented the hypothetical pathways participating in the radiosensitization of HepG2 cells and radioprotection of BRL-3A cells. The green colour indicated upregulation and red colour indicated downregulation of a specific marker under IR+EC treated condition.

CONCLUSION

Pre-treatment with Ethyl cinnamate has been shown to have a biphasic mode of action post-irradiation depending on the dose and cell type. The administration of EC eliminates tumour cells by enhancing radiation effects and shielding normal cells from the detrimental effects. The findings of this study suggest that the radio-protective effect is mostly attributable to its ability to reduce oxidative stress, regulate inflammatory responses, boost pro-survival parameters, and prevent DNA damage. In contrast, the radiosensitive activity might be due to increased oxidative stress, cell cycle inhibitors (p53 & p21), DNA damage, reduced survival factors, and suppressed angiogenesis, which decrease metastasis. More research is needed to translate the current preclinical knowledge to the clinical applications of EC in combinatorial radio-therapeutic strategies.

ACKNOWLEDGMENTS

The authors thankfully acknowledge UGC (University Grant Commission), Government of India for funding the project (Sanction no. F.15-6Dec 2014/2015 NET), and UGC-DAE Consortium for Scientific Research, Kolkata Centre, India, for providing all the facilities to conduct this research work.

***Conflicts of Interest*:** The authors declare that there are no conflicts of interest.

***Ethical consideration*:** This article does not contain any investigation with animals or human participants performed by any of the authors.

***Author contributions*:** Conceptualization was done by A.D. and A.C.; Methodology was carried out by A.D., S.M.; AD did the investigation and formal analysis; A.D. prepared the original draft; A.D.& S.M did the writing—review and editing; A.D. acquired the fund; A.D., A.C. obtained the resources; All authors reviewed the manuscript.

REFERENCES

1. Morgan WF and Sowa MB (2005) Effects of ionizing radiation in nonirradiated cells. *PNAS, **102**(40): 14127–14128.*
2. Kinoshita K, Ishimine H, Shiraishi K, Kato H, Doi K, *et al.* (2014) Cell and tissue damage after skin exposure to ionizing radiation: Short- and long-term effects after a single and fractional doses. *Cells Tissues Organs, **200**: 240-252.*
3. Burgio E, Piscitelli P, Migliore L (1971) Ionizing radiation and human health: Reviewing models of exposure and mechanisms of cellular damage. An epigenetic perspective. *International J of Environ Res and Pub Health*, ***15**(9): 1971*.
4. Mozdarani H (2012) Biological complexities in radiation carcinogenesis and cancer radiotherapy: Impact of New Biological Paradigms. *Genes*, ***3**(1): 90-114*.
5. Madan R (2020) Radiosensitizers and radioprotectors. In: Practical radiation oncology, (Mallick S., Rath G., Benson R, eds.). *Springer Singapore, 179-183*.
6. Yi J, Zhu J, Zhao C, Kang Q, Zhang X, Suo K, *et al.* (2021) Potential of natural products as radioprotectors and radiosensitizers: opportunities and challenges. *Food Funct*, **12:** 5204-5218.
7. Rates SMK (2001) Plants as source of drugs. *Toxicon, **39**(5): 603-613.*
8. Veeresham C (2012) Natural products derived from plants as a source of drugs. *J Adv Pharm Tech Res, **3**: 200-201.*
9. Greenwell M and Rahman PKSM (2015) Medicinal plants: Their use in anticancer treatment. *Int J Pharm Sci Res, **6**(10): 4103–4112.*
10. Kavishankar GB, Lakshmidevi N, Mahadeva Murthy S, Prakash HS, Niranjana SR (2011) Diabetes and medicinal plants-A review. *Int J Pharm Biomed Sci, **2**(3): 65-80.*
11. Mannangatti P, Naidu KN (2016) Indian herbs for the treatment of neurodegenerative disease. In: The benefits of natural products for neurodegenerative diseases. (Essa M., Akbar M., Guil-

[DOI: 10.52547/ijrr.21.2.1]

lemin G, eds.), Springer, Switzerland. *Advances in Neurobiology*, **12**: 323-336.
12. Pohl F and Kong Thoo Lin P (2018) The potential use of plant natural products and plant extracts with antioxidant properties for the prevention/treatment of neurodegenerative diseases: *In-vitro*, *in-vivo* and clinical trials. *Molecules*, ***23****(12): 3283*.
13. Juanjuan Yi, Jiaqing Zhu, Changcheng Zhao, Qiaozhen Kang, *et al.* (2021) Potential of natural products as radioprotectors and radiosensitizers: opportunities and challenges. *FoodFunct,* **12**: 5204–5218.
14. Reya T, Morrison S, Clarke M, *et al.* (2001) Stem cells, cancer, and cancer stem cells. *Nature, **414**: 105–111.*
15. Sagan L (1967) On the origin of mitosing cells. *J of TheoretBiol, **14** (3): 225-274.*
16. Mair W (2010) How normal cells can win the battle for survival against cancer cells. *PLoSBiol, **8**(7): e1000423.*
17. Zhang L, Zhou W, Velculescu VE, Kern SE, Hruban RH, *et al.* (1997) Gene expression profiles in normal and cancer cells. *Science*, **276** (5316): 1268-1272.
18. MYallapu M, Maher DM, Sundram V, Bell MC, Jaggi M, Chauhan SC (2010) Curcumin induces chemo/radio-sensitization in ovarian cancer cells and curcumin nanoparticles inhibit ovarian cancer cell growth. *J Ovarian Res, **3**: 11.*
19. Li M, Zhang Z, Hill DL, Wang H, Zhang R (2007) Curcumin, a dietary component, has anticancer, chemosensitization, and radiosensitization effects by down-regulating the MDM2 oncogene through the PI3K/mTOR/ETS2 pathway. *Cancer Res, **67**: (5) 1988-1996.*
20. da Costa Araldi IC, Bordin FPR, Cadoná FC, Barbisan F, *et al.* (2018) The *in-vitro* radiosensitizer potential of resveratrol on MCF-7 breast cancer cells. *Chem-Biol Interact, **282**: 85-92.*
21. Tan Y, Wei X, Zhang W, Wang X, Wang K, *et al.* (2017) Resveratrol enhances the radiosensitivity of nasopharyngeal carcinoma cells by downregulating E2F1. *Onco Rep, **37**: 1833-1841.*
22. Baek SH, Ko J-H, Lee H, Jung J, Kong M, JW Lee, J Lee, *et al.* (2016) Resveratrol inhibits STAT3 signaling pathway through the induction of SOCS-1: Role in apoptosis induction and radiosensitization in head and neck tumor cells. *Phytomedicine, **23**(5): 566-577.*
23. Sebastià N, Montoro A, Hervás D, Pantelias G, Hatzi VI, *et al.* (2014) Curcumin and trans-resveratrol exert cell cycle-dependent radioprotective or radiosensitizing effects as elucidated by the PCC and G2-assay. *Mutat Res /Fundament and MolMech of Mutagen, **766–767**: 49-55*.
24. Karthikeyan S, Kanimozhi G, Prasad NR, Mahalakshmi R (2011) Radiosensitizing effect of ferulic acid on human cervical carcinoma cells *in-vitro*. *Toxicology in-Vitro, **25**(7): 1366-1375.*
25. Rajendra Prasad N, Srinivasan M, Pugalendi KV, Venugopal PM (2006) Protective effect of ferulic acid on γ-radiation-induced micronuclei, dicentric aberration and lipid peroxidation in human lymphocytes. *Mutat Res /Gen Toxicol and Environ Mutagen, **603** (2): 129-134.*
26. Jiao Y, Ouyang HL, Jiang YJ, Kong XZ, *et al.* (2015) Toxic effects of ethyl cinnamate on the photosynthesis and physiological characteristics of chlorella vulgaris based on chlorophyll fluorescence and flow cytometry analysis. *Sci World J, **2015**: 107823.*
27. Gao LL, Guo PY, Su GM and Wei YF (2013) Effects of allelochemicals ethyl cinnamate on the growth and physiological characteristics of Chlorella pyrenoidosa. *Huan Jing KeXue, **34**(1): 156-62.*
28. Zhang B, Lv C, Li W, Cui Z, Chen D, *et al.* (2015) Ethyl cinnamate derivatives as promising high-efficient acaricides against Psoroptescuniculi: synthesis, bioactivity and structure-activity relationship. *Chem Pharm Bull, **63**(4): 255-62.*
29. Dubey NK, Tiwari TN, Mandin D, Andriamboavonjy H, Chaumont JP (2000) Antifungal properties of Ocimumgratissimum essential oil (ethyl cinnamate chemotype). *Fitoterapia, **71**(5): 567-9*
30. Beers Jr. R and Sizer I (1952) A spectrophotometric method for measuring the breakdown of hydrogen peroxide by catalase. *J BiolChem*, ***195****(1): 133-40*.
31. Mashimo M, Onishi M, Uno A, Tanimichi A, Nobeyama A, *et al.* (2021) The 89-kDa PARP1 cleavage fragment serves as a cytoplasmicPAR carrier to induce AIF-mediated apoptosis. *J Biol Chem, **296**: 100046.*
32. Grasso R, Dell'Albani P, Carbone C, Spatuzza M, *et al.* (2020) Synergic pro-apoptotic effects of Ferulic Acid and nanostructured lipid carrier in glioblastoma cells assessed through molecular and Delayed Luminescence studies. *Scientific Reports,* **10**: 4680.
33. Malik A, Afaq S, Shahid Kafil AM, Assiri A (2011) Influence of ellagic acid on prostate cancer cell proliferation: A caspase-dependent pathway. *Asian Pacific Journal of Tropical Medicine, **4**(7): 550-555*.
34. Marechal A and Zou L (2013) DNA damage sensing by the ATM and ATR Kinases. *Cold Spring Harb Perspect Biol, **5**: a012716.*
35. Chen Y-A, Lien H-M, Kao M-C, Lo U-G, Lin L-C, Lin C-J, *et al.* (2017) Sensitization of radioresistant prostate cancer cells by resveratrol isolated from *arachishypogaea*stems. *PLoS ONE, **12**(1): e0169204*.
36. Sahu RP, Batra S, SK Srivastava (2009) Activation of ATM/Chk1 by curcumin causes cell cycle arrest and apoptosis in human pancreatic cancer cells. *British J Cancer, **100**: 1425 – 1433*.
37. Kuo LJ and Yang L-X (2008) γ-H2AX – a novel biomarker for DNA double-strand breaks. *In-vivo, **22**: 305-310.*
38. Schwarz K, Dobiasch S, Nguyen L, Schilling D, Combs SE (2020) Modification of radiosensitivity by Curcumin in human pancreatic cancer cell lines. *Scientific Report, **10**: 3815*.
39. He G, Siddik ZH, Huang Z, Wang R, Koomen J, *et al.* (2005) Induction of p21 by p53 following DNA damage inhibits both Cdk4 and Cdk2 activities. *Oncogene, **24**(18): 2929-43.*
40. Jang JY, Kang MY, Lim YK, Kim JH, Kim JK (2017) Effects of quercetin on ionizing radiation-induced cellular responses in HepG2 cells. *Int J Radiat Res, **15**(3): 229-239.*
41. Li, T-M, Chen G-W, Su C-C, Lin J-G, Yeh C-C et al. (2005) Ellagic acid induced p53/p21 expression, G1 arrest and apoptosis in human bladder cancer T24 cells. *Anticancer Research, **(25)**: 971-9.*
42. Valdameri G, Trombetta-Lima M, Worfel PR, Pires ARA, Martinez GR, *et al.* (2011) Involvement of catalase in the apoptotic mechanism induced by apigenin in HepG2 human hepatoma cells. *Chem-Biol Interact, **193**: 180–189.*
43. Glorieux C, Marcelo Sandoval J, Dejeans N, Nonckreman S, Bahloula K, *et al.* (2018) Evaluation of potential mechanisms controlling the catalase expression in breast cancer cells. Oxid Med Cell Longev, 10: 1155/2018/5351967.
44. Subburayan Karthikeyan, Govindhasamy Kanimozhi, Nagarajan Rajendra Prasad, Rajendran Mahalakshmi(2011) Radiosensitizing effect of ferulic acid on human cervical carcinoma cells *in-vitro*. *Toxicology In-Vitro, **25**: 1366–1375*.
45. Wagner E and Nebreda A (2009) Signal integration by JNK and p38 MAPK pathways in cancer development. *Nat Rev Cancer, **9**: 537–549.*
46. Tang Y, Abe N, Qi H, Zhu B, *et al.* (2014) Tea catechins inhibit cell proliferation through hydrogen peroxide- dependent and -independent pathways in human t lymphocytic leukemia Jurkat cells. *Food Science and Technology Research, **20** (6): 1245_1249*.
47. Zhang Y, Chen P, Hong H, Wang L, Zhou Y, Lang Y (2017) JNK pathway mediates curcumin-induced apoptosis and autophagy in osteosarcoma MG63 cells. *Experimental and Therapeutic Medicine, **14**: 593-599*.
48. Thomas S, Snowden J, Zeidler M, *et al.* (2015) The role of JAK/STAT signalling in the pathogenesis, prognosis, and treatment of solid tumours. *Br J Can, **113:** 365–371.*
49. Zhong L-X, Zhang Y, Wu M-L Liu, Y-N, Zhang P, *et al.* (2016) Resveratrol and STAT inhibitor enhance autophagy in ovarian cancer cells. *Cell Death Discovery, **2**: 15071*.
50. Madan E, Prasad S, Preeti R (2008) Regulation of apoptosis by resveratrol through JAK/STAT and mitochondria mediated pathway in human epidermoid carcinoma A431 cells. *Biochemical and Biophysical Research Communications, **377:** 1232–1237*.
51. Xia Y, Shen S, Verma IM (2014) NF-κB, an active player in human cancers. *CanImmunol Res, **2**(9): 823–830.*
52. Xia L, Tan S, Zhou Y, Lin J, Yang H, Oyang L, *et al.* (2018) Role of the NFκB-signaling pathway in cancer. *Onco Target and Ther, **11**: 2063-2073.*
53. Zinatizadeh Md R, Schock B, Chalbatani GM, Zarandi PK, *et al.* (2021) The Nuclear Factor Kappa B (NF-kB) signaling in cancer development and immune diseases. *Genes & Diseases, **8**: 287-297.*
54. Marquardt JU, Gomez-Quiroz L, Arreguin Camacho LO, Pinna F, *et al.* (2015) Factor, and Snorri S. Curcumin effectively inhibits oncogenic NF-kB signaling and restrains stemness features in liver cancer. *Thorgeirsson J Hepatol, **63**(3): 661–669*.
55. Peeney D, Jensen SM, Castro NP, Kumar S, Noonan S, Handler C, *et al.* (2020) TIMP-2 suppresses tumor growth and metastasis in murine model of triple-negative breast cancer. *Carcinogenesis, **41** (3): 313–325.*
56. Wang W, Li D, Xiang L, Lv M, Tao L, Ni T, *et al.* (2019) TIMP-2inhibits metastasis and predicts prognosis of colorectal cancer via regulating MMP-9. *Cell Adhesion & Migration, **13**(1): 272-283.*
57. ShiJ, Zhang X, Shi T, Li H (2017) Antitumor effects of curcumin in human bladder cancer *in-vitro. Oncology Letters, **14**: 1157-1161*.

[DOI: 10.52547/ijrr.21.2.1]